Mine Closure 2023 - Behrooz Abbasi, Jeff Parshley, Andy Fourie & Mark Tibbett (eds)

Cold joints and hot pours in the arctic: design, implementation; and post construction investigation of a remotely placed Self Consolidating Concrete sill pillar

RP Preston *WSP, Canada*

AL Pakula *WSP, Canada*

C MacInnis *Crown Indigenous Relations and Northern Affairs Canada, Canada*

Abstract

In 2018, approximately 17,000 m3 of Self-Consolidating Concrete (SCC) was placed into a historic mining stope approximately 120 m below surface as part of long-term stabilization efforts at the Giant Mine Remediation Project. Quality control and quality assurance materials testing as well as remote monitoring of the placement concluded that the SCC met design specifications and did not settle or experience undue thermal stress during placement. However, due to logistical issues during placement interrupting the planned continuous pour, the potential for cold joints within the monolithic pour were identified. In 2021, the artificial sill pillar was drilled and cored through four holes. UCS samples were collected; and the core was logged in support of updated modelling and assessment of the integrity of the pillar. This paper presents the results of this investigation and makes conclusions regarding the long-term performance of this monolithic, remotely constructed, sill pillar.

Keywords: *sill pillar, self-consolidating concrete, cold joints, arctic construction*

1 Introduction

The Giant Mine Remediation Project is located approximately 5 km north of the city of Yellowknife, NWT at the site of the former Giant Mine (Figure 1). The Giant Mine operated from the late 1940s to 2004 at which time the mine went into care and maintenance under the ownership of the Government of Canada (Silke 2009). The mining was primarily underground using a variety of stoping methods, but eight open pits were also excavated, relatively late in the mine life. The roasting process to extract gold resulted in the creation of 237,000 t of arsenic trioxide dust which are currently stored underground in a combination of previously mined stopes and purpose excavated storage chambers.

Figure 1 Location of Giant Mine (Google n.d.)

During investigations and analysis in support of long-term closure planning it was identified that the C509 stope complex posed an unacceptable risk of crown pillar failure which could result in arsenic trioxide release from the overlying arsenic storage stope (C212) and chambers (C9, C10) (Figure 2). The C509 stope complex had previously been backfilled with run of mine material but in 2007 during a raise in mine water level, approximately 170,000 t of fill displaced out of the stope and moved deeper into the mine. This resulted in a large open void measuring approximately 70 m long by 22 m wide by 40 m high (Figure 3). The stope complex was investigated through a combination of underground inspections, drilling and borehole camera surveys, Cavity Monitoring System Surveys and unmanned aerial vehicle surveys (Preston & Roy 2017, Pakula et al. 2019) in 2016.

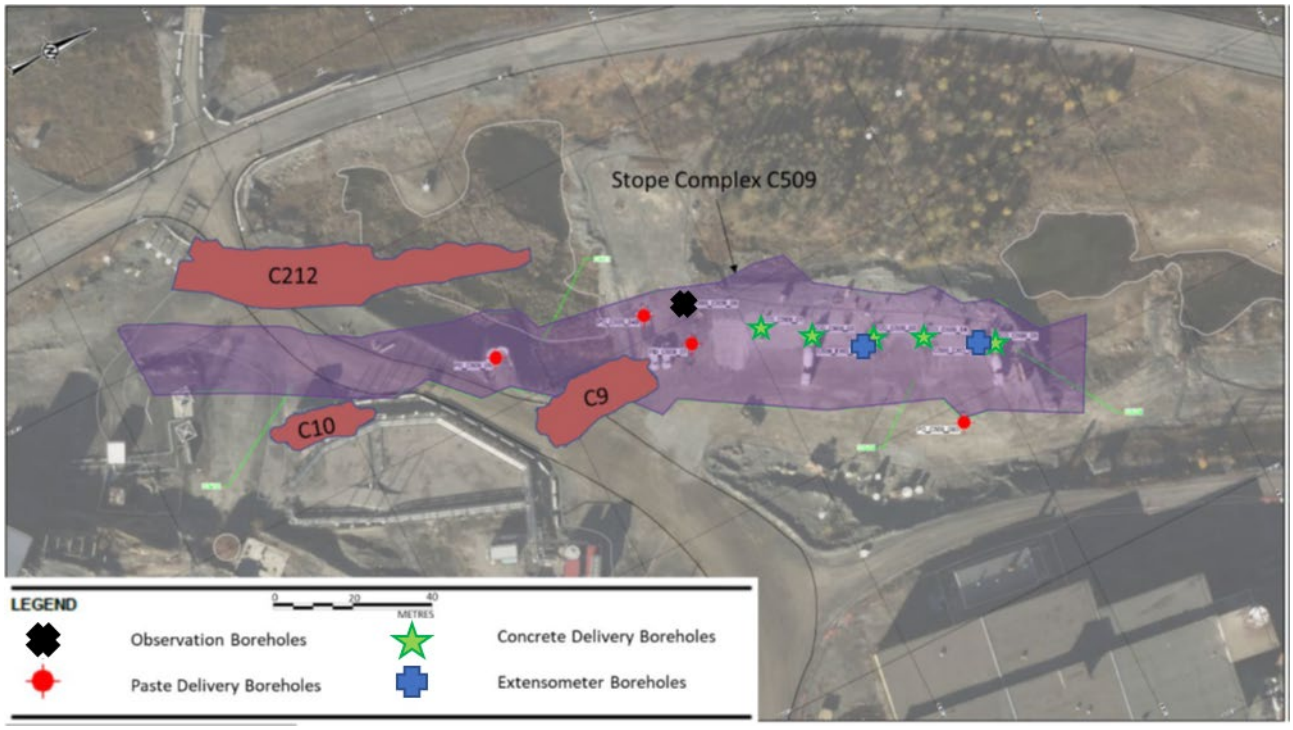

Figure 2 Plan view of surface projection of arsenic stope and chambers (red) and C509 non-arsenic stope complex (purple) with relevant boreholes (after Pakula et al 2019)

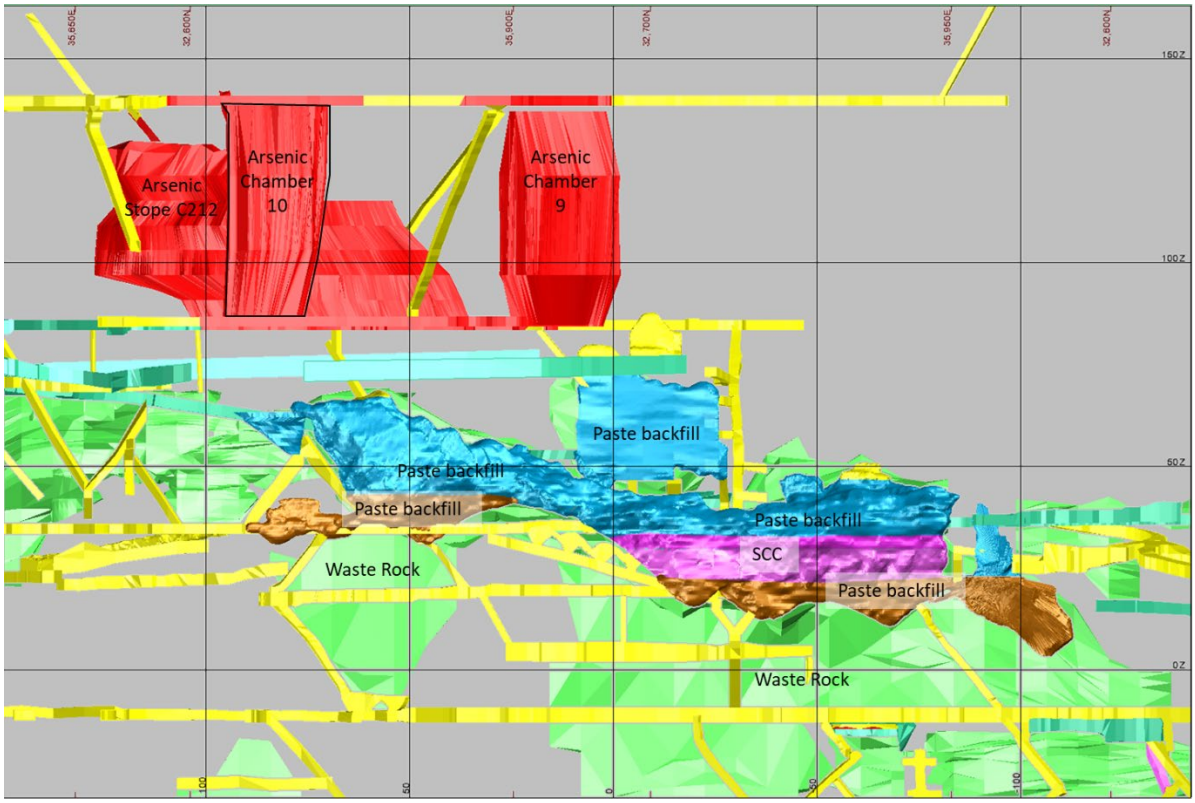

Figure 3 Long section view looking west of C509 stope complex and overlying arsenic storage. SCC sill pillar and paste backfill shown as well as historical waste rock

2 Design

Following conclusion of the initial investigations in 2016, a design was developed to backfill the C509 stope complex to provide support to the crown pillar in the event the underlying backfill were to evacuate again. Based on the assessed risk of further historical fill displacement, it was necessary to design the new backfill to be self-supporting in the event that it was undermined by future historical fill instability. The chosen approach was to place a 10 m thick plug of self-consolidating concrete within the void at an elevation where the geometry of the stope would cause it to have good contact with the side walls (Pakula et al. 2019). This required placing a layer of cemented tailings paste backfill (CPB) onto the existing fill to produce a level working platform for the constructed sill pillar and allow it to be placed at the design elevation. The remainder of the void above the sill pillar was also designed to be backfilled with cemented tailings paste to reduce the remaining void volume and support the crown pillar (Figure 3).

The sill pillar was designed to be placed between 141 and 151 mbgs where the stope geometry was favourable, i.e. the ribs sloped inwards and rock walls were available on three of four sides. The initial design thickness of the sill pillar was confirmed through 2D finite element modelling conducted over 12 representative cross sections along the strike of the sill pillar to account for variability in the stope wall profile and under three different loading scenarios. The loading scenarios were: low load (cemented backfill), moderate load (uncemented backfill) and high load (crown pillar failure or hanging wall sliding failure) (Figure 4). The section shown below was determined to be one of the critical ones due to the width of the stope and relatively vertical side wall with some overhangs. Modelling showed that under all three loading conditions, a zone of tensile stress would form in the bottom middle of the sill pillar. Therefore, progressive tensile cracking was modelled by extending the crack upwards until compressive stresses were found at the crack tip. It was found that a crack would extend but only part way before it closed off and the sill pillar would be self-supporting, provided it was constructed in a monolithic manner (no joints).

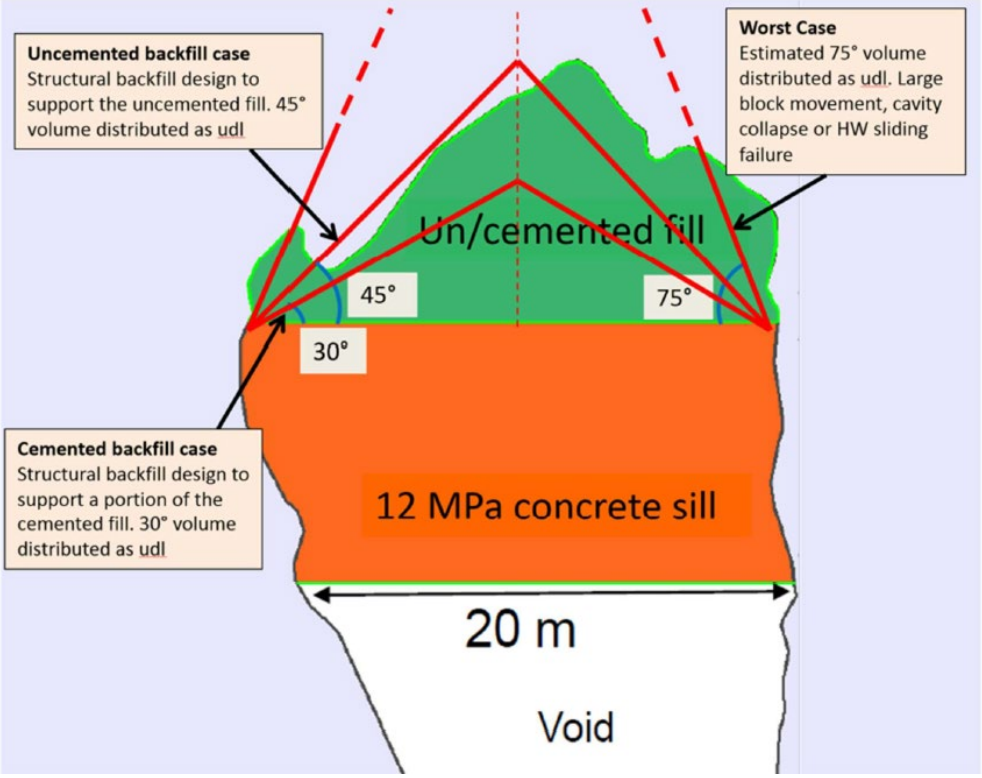

Figure 4 **Critical cross section modelled as part of SCC pillar design showing assumed void below SCC and three loading scenarios accounting for potential backfill conditions above the SCC**

3 Construction

Construction of the SCC sill pillar was completed between 20 September 2018 and 21 October 2018 by Nahanni Construction Ltd. Interruptions to the supply of cement binder was identified as a project risk as the pour needed to be continuous to prevent cold joints from forming.

The sill pillar was placed using five boreholes spaced out along the strike of the void and drilled from surface. They were initially planned to be used as tremie pipes but during placement it was found that the skin friction in the pipe was too high, and the tremies were raised just above the backfill surface and the SCC was free poured resulting in splash pools at the base of the tremies. To maintain a live surface over the entire sill at all times, the SCC was placed sequentially between the five pipes and allowed to reach the edges of the stope before switching pipes. This required production rates between 12 and 34 m^3/hr based on the 18-23 hour set time of the SCC determined by laboratory testing during placement.

Monitoring was conducted using a combination of infrared pan-tilt-zoom cameras installed within the void and connected to a surface monitoring area with real time viewing, extensometers with thermistors within the centre of the void and, plumb bobs on the edges of the void (Figure 6). Cavity Monitoring System (CMS) scans were also taken periodically.

Unfortunately, nine days into pouring supply of the original T90/10 cement binder became limited and pouring rates were reduced in an effort to maintain a live SCC surface while a replacement cement binder was trialled and an updated mix design developed. Rates were further slowed on 2 October 2018 as the supply of cement started to reach critical low levels and, at that time, concerns were raised that a live leading edge may not have been maintained. These concerns were based on plumb bob observations that indicated no rise in the SCC level at the measured locations on the stope edge over two separate 24 hour periods and, observations of channels forming in the SCC flow paths following relatively long breaks in pouring (Figure 5). On 8 October 2018, the project switched cement binders from the T90/10 to using the Sundance 70/30 following completion of site trial tests and used Sundance for the remainder of the SCC pour (Pakula et al. 2019).

Figure 5 **Footage from underground infrared camera showing splash pool under tremie pipe. Extensometer string with reflective tape shown in foreground of tremie pipe and braided flow channels in SCC**

4 Post construction investigation

Following completion of construction and the identification of the potential for cold joints to have formed during the transition between cement binders, an investigative drilling program was designed. Four core holes were drilled through the SCC plug with the intention of characterizing the SCC in four locations; near the edge of the plug, in the path of a SCC delivery hole and at both the north and south ends of the stope (Figure 6).

Four triple tube, HQ3 core holes were completed in the summer of 2021. Core was retrieved through all three layers of backfill (paste-SCC-paste) and the holes were terminated once the underlying historic backfill or the intact rock wall were reached, depending on their orientation (Figure 6). Paste and SCC core recovery was successful over the entire hole lengths and, was generally 100% in the SCC layer. Continuous core retrieval through the underlying paste and into the underlying bedrock or historical backfill and subsequent borehole camera survey data was interpreted to indicate that there are no significant voids underneath the 2018 backfill. This is corroborated by extensometer data which indicated approximately 1 mm of compression during construction and have since exhibited a gradual trend of extension towards zero total displacement, likely associated with cooling of the plug.

The boreholes were surveyed with a borehole camera following drilling. Borehole camera footage in all boreholes recorded an interpreted intact/closed contact between the SCC and adjoining paste (both upper and lower) and between the two different layers of SCC when the binder transitioned. Finally, the observed thickness and elevation of the paste and SCC layers matched expectations based on pouring records.

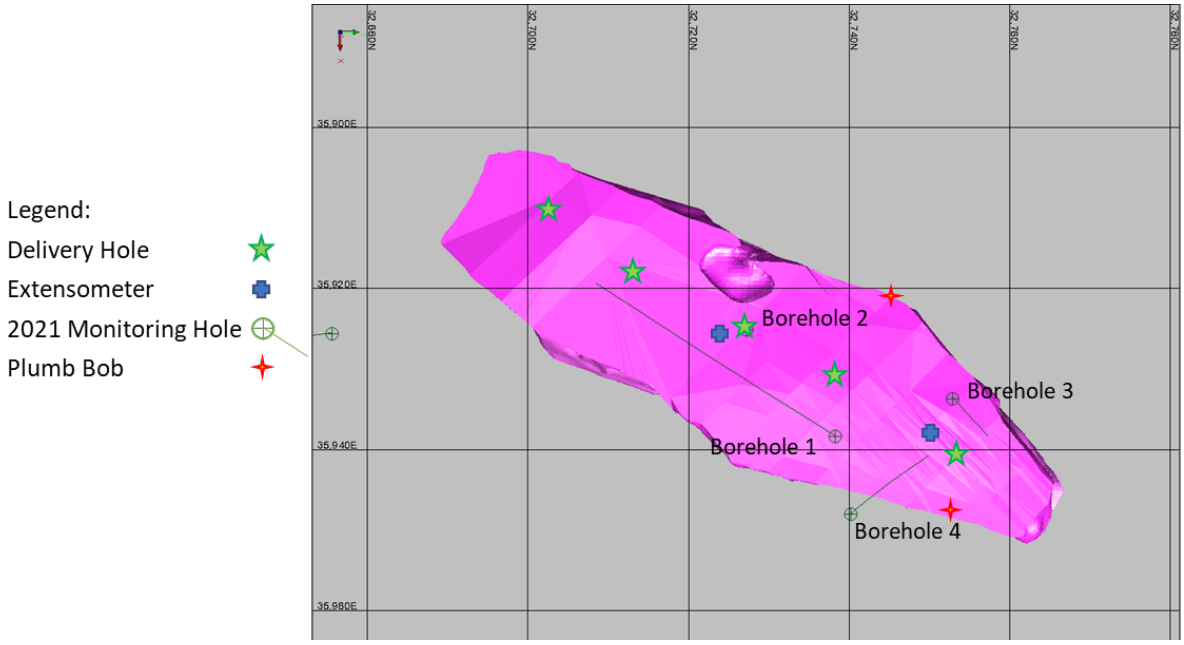

Figure 6 Plan view of mine model showing top of SCC plug with key locations highlighted

4.1 Identification of discontinuities

Following retrieval of the core, all breaks within the SCC zone were reviewed by WSP personnel to identify potential cold joints. In Borehole 1, three interpreted cold joints were identified and subsequently correlated with borehole camera records (Figure 7). In Borehole 3 and Borehole 4, no obvious cold joints with corresponding smooth surfaces were initially identified from core logging, but an obvious fracture was identified in each of the borehole camera records (Figures 8 and 9).

Figure 7 Interpreted cold joint in box (left), split to expose surfaces (centre) and in borehole camera video (right) from borehole 1 at ~138.7 m along hole/30.24 mamsl

Figure 8 **Interpreted cold joint in box (left), split to expose surfaces (centre) and in borehole camera video (right) from borehole 3 at 136.8 m along hole/ 27.18 mamsl**

Figure 9 **Interpreted cold joint in box (left), split to expose surfaces (centre) and in borehole camera video (right) from borehole 4 at 136.9 m along hole/28.01 mamsl**

No discontinuities were identified in the core or camera footage from Borehole 2, which was drilled through the concrete delivery hole CD_03. However, areas of increased porosity resulting in mechanical fractures of the core were observed, which may have been associated with the splash pool formations observed from infrared camera footage during placement (Figures 5 and 10).

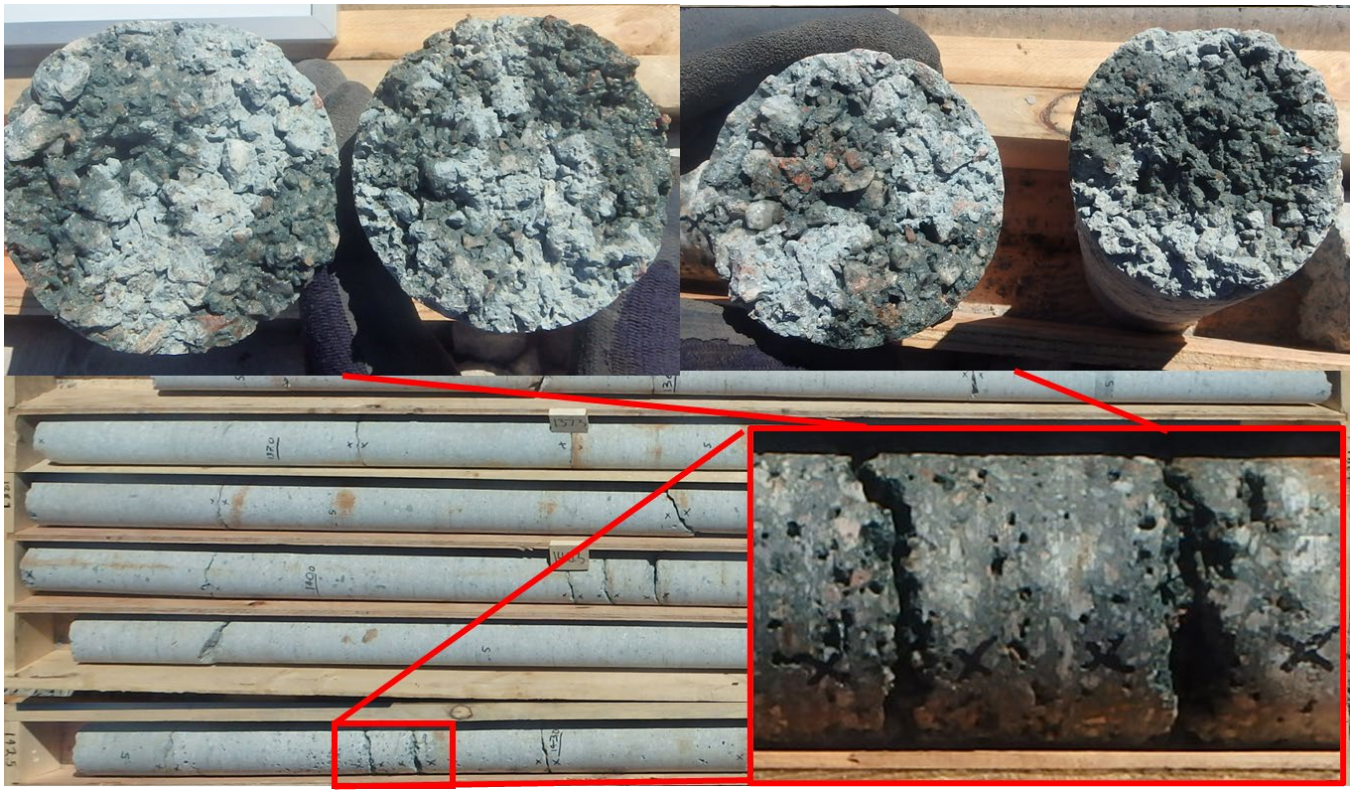

Figure 10 Interpreted porosity induced mechanical fractures in core from borehole 2

The identified cold joints are shown in section view of the SCC plug in Figure 11 as well as the thickness of the plug and the depth of the highest cold joint identified relative to the top of SCC.

SCC elevations were regularly measured at the two extensometers and the underground plumb bobs and, can be roughly correlated to the elevation of the cold joints observed. However, as shown by CMS data, the SCC surface was not perfectly level and, as the 2021 monitoring holes were not drilled directly below either of the plumb bobs, it is difficult to conclusively correlate the elevation of a given feature in a borehole with a given day of pouring. In addition, there is likely to be variable degrees of error and uncertainty in the given measurement methods, i.e., core/borehole camera depth and plumb bob measurements. Therefore, elevations of features of interest in the monitoring holes were interpreted to be accurate to approximately +/- 0.5 m. Table 1 summarizes the identified joints and their best correlation with pouring records summarized in Section 3. As shown, with the exception of one joint in Borehole 1, all joints correlate reasonably well to the pouring records. The lack of correlation can likely be explained by Borehole 1's greater distance from known reference points compared to the other three holes.

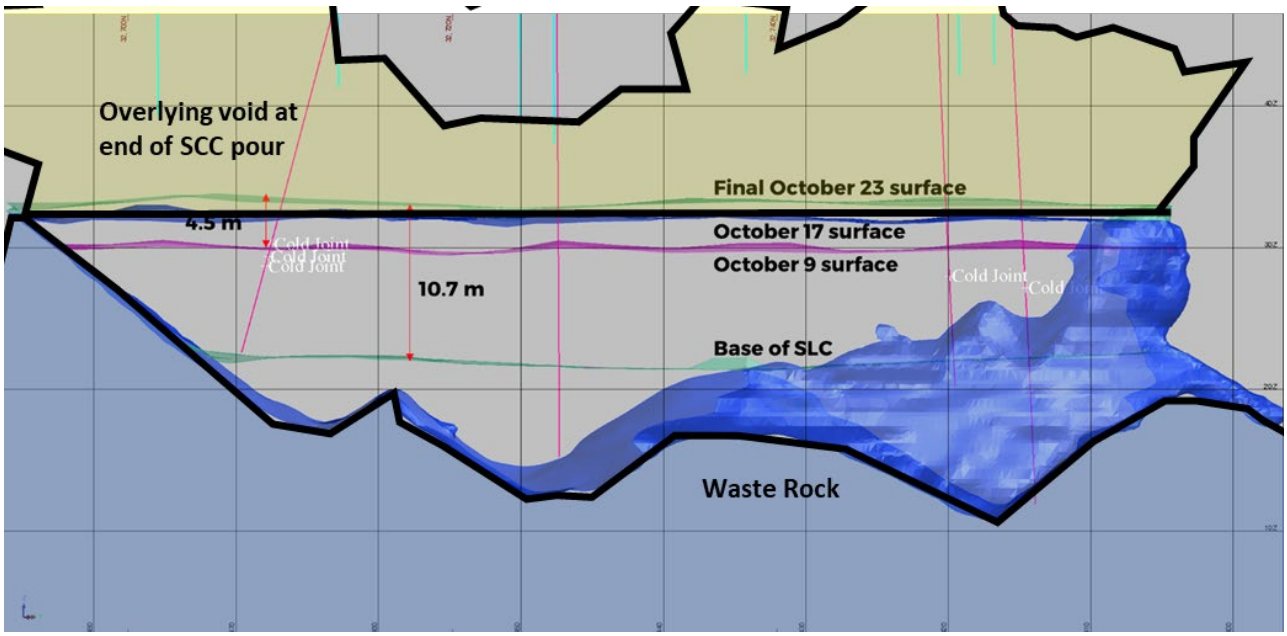

Figure 11 Section view looking west of SCC plug and underlying paste topography of C509 with identified cold joints (white) plotted along borehole paths. October 9 surface corresponds to transition in binder type, October 17 is an intermediate surface illustrating variations in elevation along strike and October 23 is end off SCC pouring

Table 1 Summary of identified cold joints and correlation to pouring records

Borehole	Borehole Location	Description	Depth Along Hole	Elevation (mamsl)	Pouring Records Correlation
Borehole 1	South end near CD_02	Smooth cold joint in core and confirmed from borehole camera.	138.7	30.2	11 Oct., preferential flow paths noted
			139.6	29.4	Approx. 7 Oct., no direct correlation
			140.3	28.7	5 Oct., no rise at ballroom plumb bob
Borehole 3	Relative high point near CD_05	Rough fracture in core, confirmed from borehole camera	136.8	27.2	Approx. 1 Oct., Between periods of no rise at plumb bobs
Borehole 4	Relative low point near CD_05, Exo_02 and Ballroom plumb bob	Mixed rough and smooth fracture in core, confirmed from borehole camera	136.9	28.0	3 Oct., no rise at FB-6 plumb bob

4.2 Laboratory strength testing

Twenty core samples were retrieved from the four boreholes, five from each hole, roughly evenly spaced across the borehole intersection of the SCC and tested for Unconfined Compressive Strength. All samples

were found to exceed the 12 MPa design strength with an average strength of approximately 37 MPa and a minimum strength of 22.5 MPa. The strength of the upper Sundance layer was found to be more variable and, because it represented a smaller percentage of the actual plug, fewer samples were collected.

5 Interpretation of investigation findings

The joints identified both in core and borehole camera records were found to correspond to the period in early October 2018 when SCC pouring rates were reduced due to supply limitations of cement binder and are interpreted to be cold joints. With the limited number of investigation boreholes drilled through the SCC plug, it is difficult to state conclusively what the continuity of these fractures is likely to be. With evidence from Borehole 2 that cold joints were not formed directly underneath concrete delivery holes it is unlikely that the observed fractures traverse the entire width or length of the plug. However, evidence from Borehole 3 and Borehole 4, which were drilled within approximately 5 m of delivery hole CD_05 suggest that jointing due to interruptions to flow of SCC to a specific area is possible relatively close to a delivery hole. As shown in Figure 5, the flow pattern was not consistently perfectly radial so it is possible that the cold joint areas did not receive fresh SCC but areas immediately adjacent received fresh SCC regularly and therefore did not form a joint.

6 Modelling

Based on the findings of the investigation that cold joints of unknown persistence were present, it was considered prudent to revise the numerical modelling completed in support of the initial design to review the potential impacts of varying continuities of cold joints at the elevation observed as the initial modelling had indicated that the pillar would need to be massive to function as intended in the event the underlying fill evacuated in the future.

The previous model of a critical section was revised for the cold joint geometry and for the in-situ UCS strength obtained from lab testing. The same low, moderate and high loading cases from the original model were carried forward. For the modelling a design strength was determined using the 5% fractile of the log normal strength distribution with a material safety factor and specific situation modifier applied. Because there were only 9 samples from the Sundance with high variability in results, the 5% fractile was lower than the T90/10. The potential to expand the strength data set based on 7 and 28 day UCS strengths from the field was reviewed but, it was found that the SCC did not follow normal concrete time strength curves so extrapolation to 3 year strengths was not considered valid. The resulting modelled compressive and tensile strengths were 19 MPa and 1.26 MPa for the T90/10 layer and 9.13 and 0.68 MPa for the Sundance layer.

For modelling, cold joints were interpreted to be fully continuous at 4.5 m below the top of the SCC (the highest cold joint observed), leaving a 6 m thick T90/10 layer below. The 4.5 m thick layer was modelled as all Sundance. Vertical tension cracks were modelled and the cold joint was modelled as compression only (no shear or tensile strength). The rock-SCC contact was modelled as perpendicular compression only springs (no friction) (Figure 12). For comparison, the same model was run but with the binder layer bonded to isolate the impact of the cold joint. The vertical crack was iteratively expanded until it was found that the tip was under compressive stress. The length of the tension crack was checked for the three load cases and was found to be longer for the higher load case, as expected.

Because of the overhangs on both side walls, which were most pronounced on the right wall, limited areas of the side walls were available for bearing capacity in the lower, thicker T90/10 layer (Figure 12). It was found that for the moderate load (Figure 13) and high load cases, tensile yielding was expected on the side wall contacts in the T90/10. No compressive yielding was noted for any of the loading cases. The tensile yielding indicates the potential for a horizontal joint to form and the lower right part of the SCC to drop off;

however, the remaining part should be stable and support the load based on modelled stress conditions. Deformation of the SCC was predicted as 4.3 mm surface dip for the high loading case.

The revised modelling does not account for the 3D nature of the constructed sill or the smaller scale roughness of the wall stope walls. Tension cracks in the middle of the pillar and yield zones on the side walls did not extend to the top of the slabs even in the most conservative modelled loading case. The yielded zone (Figure 13) was also below the shoulder where the SCC was able to mobilize its strength (Figure 12) and it is interpreted that the loss of that material wouldn't have an impact on the load bearing capacity of the remaining material.

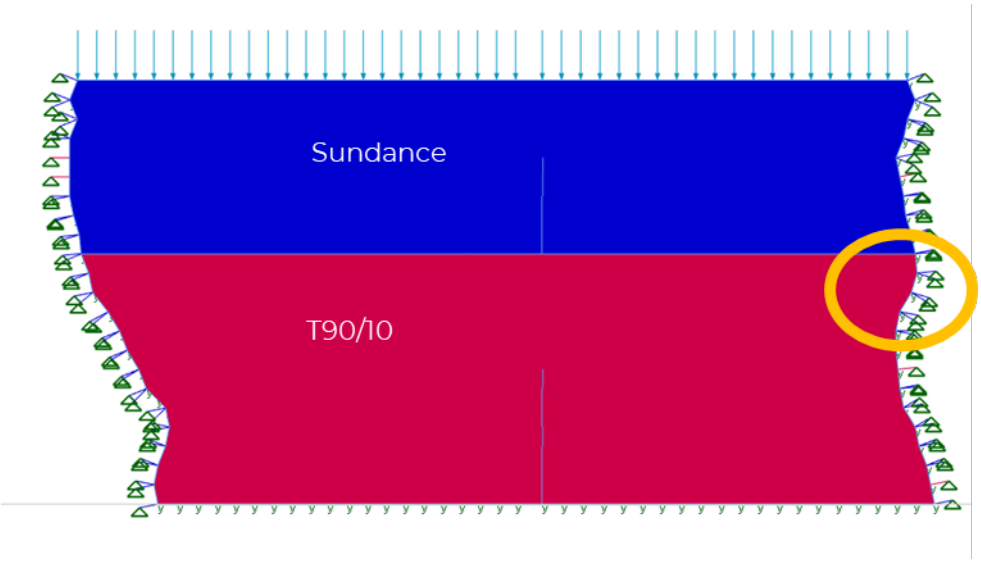

Figure 12 Revised finite element model of SCC plug showing T90/10 and Sundance layers with tension cracks in the centre of each and the area of bearing capacity on the right side wall (orange circle)

The bonded model (no cold joint), under the high loading case exhibited some tensile yielding in the lower T90/10 layer and a dip of approximately 1.7 mm was predicted in the centre of the pillar.

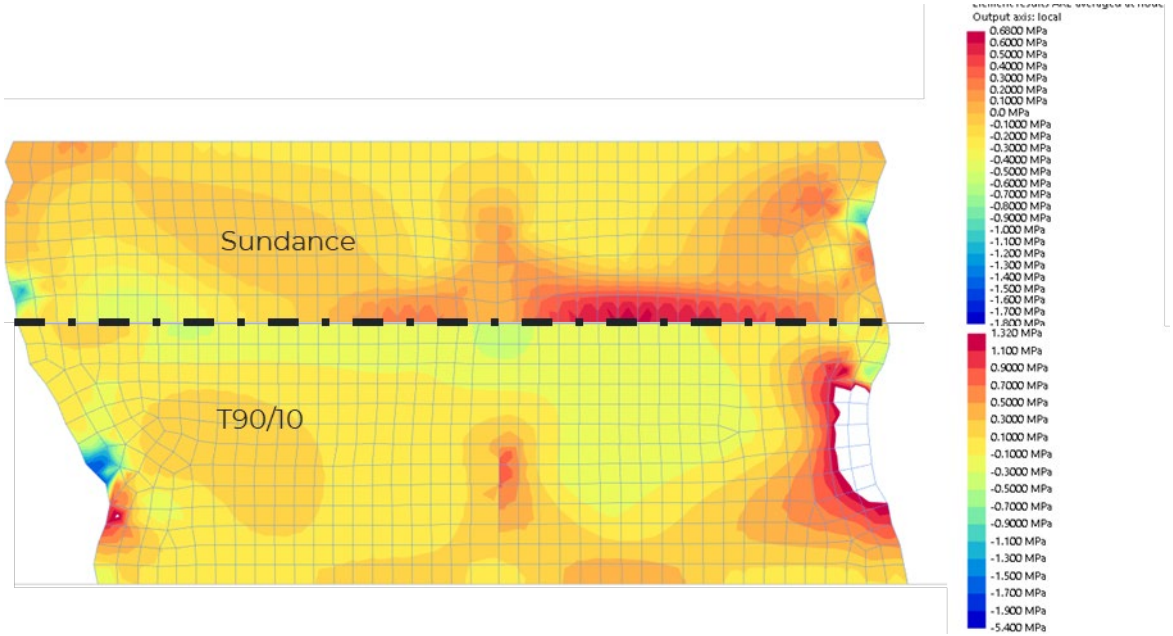

Figure 13 Modelled tensile stresses for moderate load (uncemented backfill) load case showing potential tensile failure in right side wall of T90/10 layer

This modelling included several conservative assumptions and simplifications. The rock concrete interface was modelled as frictionless because data were not available but qualitative observations of side wall roughness suggest that some frictional strength would be present. Similarly, although the cold joints were observed to be smooth in some cases (Figure 7), they were not uniformly smooth (Figures 8 and 9) and, even so, would be expected to exhibit some frictional strength if not some cohesion due to their likely discontinuous nature. Similarly, the cold joint layer was modelled as fully continuous, which cannot be ruled out, but is unlikely based on the balance of available data. The modelled moderate and high loading cases are also likely conservative as cemented paste backfill was placed above the SCC and is expected to support the overlying crown pillar to prevent large scale failure. Finally, approximately 50% of reviewed sections through the C509 void were found to have the less favourable, overhanging side wall geometry, which means that another 50% are more favourably shaped and should mobilize more strength with reduced zones of yielding.

7 Conclusion

A review of borehole camera data and retrieved core from investigation boreholes confirmed the presence of cold joints in three of four holes with an elevation range of 30.2 to 27.2 m masl within the SCC layer. These joints correspond to the period during which delivery of the SCC was slowed as a result of cement binder supply issues. Based on the limited available spatial data, it was not possible to draw conclusions about the lateral extents of these discontinuities.

Modelling of the SCC plug at a critical representative section concluded that large-scale failure is unlikely despite conservative assumptions. It is interpreted that the SCC plug will likely perform as designed at most sections and additional investigations or literature review to refine conservative assumptions are not required. The C509 void and SCC pillar continue to be monitored as part of closure works. However, it is concluded that an increased risk of failure due to the cold joints was not present.

Acknowledgement

The authors would like to thank Crown-Indigenous Relations and Northern Affairs Canada, the owners of the site, Public Services and Procurement Canada, stewards of the site and Nahanni Construction Ltd., the contractor who constructed the sill pillar.

References

Google n.d., Giant Mine, https://www.google.com/maps

Pakula, A., Preston, R., Kennard, D., & MacInnis, C. (2019, September). Stabilising an underground void: monolithic construction using self-consolidating concrete. In Mine Closure 2019: Proceedings of the 13th International Conference on Mine Closure (pp. 263-274). Australian Centre for Geomechanics.

Preston, R & Roy, J 2017, 'Use of unmanned aerial vehicles to supplement conventional investigation methods for underground open void stability and mitigation', in Y Potvin & M Hudyma (eds), Proceedings of the First International Conference on Underground Mining Technology, Australian Centre for Geomechanics, Perth, pp. 609–616.

Silke, R 2009, The Operational History of Mines in the Northwest Territories, Canada, viewed 8 April 2019, http://www.miningnorth.com/_rsc/site-content/library/NWT_Mines_History_RSilke2009.pdf